



Vtc5 Is Localized to the Vacuole Membrane by the Conserved AP-3 Complex to Regulate Polyphosphate Synthesis in Budding Yeast

Amanda Bentley-DeSousa,^{a,b}  Michael Downey^{a,b}

^aDepartment of Cellular and Molecular Medicine, University of Ottawa, Ottawa, Ontario, Canada

^bOttawa Institute of Systems Biology, University of Ottawa, Ottawa, Ontario, Canada

ABSTRACT Polyphosphates (polyP) are energy-rich polymers of inorganic phosphates assembled into chains ranging from 3 residues to thousands of residues in length. They are thought to exist in all cells on earth and play roles in an eclectic mix of functions ranging from phosphate homeostasis to cell signaling, infection control, and blood clotting. In the budding yeast *Saccharomyces cerevisiae*, polyP chains are synthesized by the vacuole-bound vacuolar transporter chaperone (VTC) complex, which synthesizes polyP while simultaneously translocating it into the vacuole lumen, where it is stored at high concentrations. VTC's activity is promoted by an accessory subunit called Vtc5. In this work, we found that the conserved AP-3 complex is required for proper Vtc5 localization to the vacuole membrane. In human cells, previous work has demonstrated that mutation of AP-3 subunits gives rise to Hermansky-Pudlak syndrome, a rare disease with molecular phenotypes that include decreased polyP accumulation in platelet dense granules. In yeast AP-3 mutants, we found that Vtc5 is rerouted to the vacuole lumen by the endosomal sorting complex required for transport (ESCRT), where it is degraded by the vacuolar protease Pep4. Cells lacking functional AP-3 have decreased levels of polyP, demonstrating that membrane localization of Vtc5 is required for its VTC stimulatory activity *in vivo*. Our work provides insight into the molecular trafficking of a critical regulator of polyP metabolism in yeast. We speculate that AP-3 may also be responsible for the delivery of polyP regulatory proteins to platelet dense granules in higher eukaryotes.

IMPORTANCE Long polymers of inorganic phosphates called polyphosphates are ubiquitous across biological kingdoms. From bacteria to humans, they have diverse functions related to protein homeostasis, energy metabolism, and cell signaling. In this study, we provide new insights into the intracellular trafficking of the polyphosphate biosynthetic machinery in the budding yeast *S. cerevisiae*. The critical advances of the work are 2-fold. First, it provides an explanation for decreased polyphosphate levels observed in cells mutated for a conserved intracellular trafficking machine. Second, it defines critical pathways that are highly likely to serve as hubs for polyphosphate regulation in yeast and other species.

KEYWORDS AP-3 complex, Apl5, Vtc5, polyP, vacuole, Pep4, ESCRT, VTC complex, *S. cerevisiae*, budding yeast, polyphosphate

Polyphosphates (polyP) are chains of inorganic phosphates found in all cell types studied to date. PolyP chains are variable in size, ranging from 3 units to thousands of units in length, and are linked together via high-energy phosphoanhydride bonds (1). While they were once dismissed as “molecular fossils,” recent work suggests that polyP plays critical roles in diverse processes across both prokaryotic and eukaryotic organisms, including bacterial virulence, infection control, blood coagulation, protein

Citation Bentley-DeSousa A, Downey M. 2021. Vtc5 is localized to the vacuole membrane by the conserved AP-3 complex to regulate polyphosphate synthesis in budding yeast. *mBio* 12:e00994-21. <https://doi.org/10.1128/mBio.00994-21>.

Editor Julia Ruth Köhler, Boston Children's Hospital

Copyright © 2021 Bentley-DeSousa and Downey. This is an open-access article distributed under the terms of the [Creative Commons Attribution 4.0 International license](https://creativecommons.org/licenses/by/4.0/).

Address correspondence to Michael Downey, mdowne2@uottawa.ca.

Received 2 April 2021

Accepted 19 August 2021

Published 21 September 2021

The original supplemental material files Fig. S1 to S4 have been revised. Revised supplemental material was posted online 5 October 2021.

folding, and diverse aspects of cell signaling (2–7). As such, polyP chains have gained significant interest as a potential target for therapeutics in a wide variety of pathologies. In contrast to bacteria and fungi, the enzymes that synthesize polyP chains in higher eukaryotic cells are largely unknown. There are no clear homologs of either prokaryotic or fungal polyP synthetases in mammals. Recent work by the Abramov group suggests that the mammalian mitochondrial F_0F_1 ATPase has polyP synthesis capabilities (8), but the overall contribution of this enzyme to total cellular pools of polyP remains to be tested.

One model organism used to study polyP at a foundational level is the budding yeast *Saccharomyces cerevisiae*. Here, polyP is present in high concentrations (>200 mM), and the enzymes responsible for its metabolism have been identified (9–11). In yeast, polyP is synthesized by the vacuolar transporter chaperone (VTC) complex. The minimal (core) VTC complex is composed of 3 subunits: Vtc1, Vtc2, or Vtc3, and the catalytic subunit Vtc4 (9, 12). The Vtc3 subunit mostly localizes to the vacuole membrane alongside Vtc1 and Vtc4 (12). On the other hand, the Vtc2 subunit is found at the endoplasmic reticulum and/or cell periphery and relocates to the vacuole membrane under phosphate-limited conditions (12). PolyP synthesis by VTC requires simultaneous translocation of polyP into the vacuole lumen (13), where it makes up over 10% of the dry weight of the cell (10). PolyP is also found in lower concentrations in the cytoplasm, plasma membrane, mitochondria, and nucleus, although observed concentrations vary by method of analysis (14). In addition to being the only known polyP synthetase in yeast, the VTC complex has been demonstrated or suggested to play a role in a myriad of cellular activities, such as the stability of vacuolar V-ATPase subunits, vacuole fusion, and microautophagy (15–17). PolyP itself has also been implicated in the regulation of pH balance (18), ion homeostasis (19–21), and phosphate metabolism (18, 22–24).

Recent work identified several exciting aspects of VTC regulation. First, activity of the complex is promoted by binding of inositol pyrophosphate InsP7 to the SPX domains of VTC proteins (25, 26). As such, loss of Kcs1, which catalyzes the formation of InsP7, drastically reduces polyP levels (27, 28). Although canonical (serine/threonine) phosphorylation and lysine ubiquitylation sites have been identified on multiple VTC subunits (29–31), their functions are currently unknown. Recently, a new VTC regulatory subunit termed Vtc5 was identified (22) (Fig. 1A, left). Vtc5 localizes exclusively to the vacuole membrane and interacts with the VTC complex to increase the rate of polyP production (22). PolyP levels in *vtc5*Δ mutants are reduced to 20% of those of wild-type cells (22). The mechanism by which Vtc5 exerts its positive effects on VTC is unknown, although it appears to function independently of effects imparted by inositol pyrophosphates (22). Given the importance of Vtc5 as a regulator of the core VTC complex, we sought to identify the pathways that are responsible for localizing Vtc5 to the vacuole membrane.

Membrane proteins are synthesized by ribosomes at the endoplasmic reticulum and transported to the trans-Golgi network (TGN) prior to being sorted to their final destination (32). Vacuolar proteins are sorted by two well-established protein transport pathways, the CPY (indirect; carboxypeptidase Y) and AP-3 (direct; adaptor protein complex 3) transport pathways (Fig. 1A, right). The CPY pathway transports cargoes to the vacuole in an indirect fashion using the endosomal system as an intermediate path. In this pathway, cargoes localize to endosomes prior to fusion with the vacuole membrane for delivery (32). In contrast, AP-3 cargoes are selected at the TGN, where the complex buds from the TGN with its cargoes to create AP-3 coated vesicles. These vesicles are transported directly to the vacuole through the cytoplasm, and AP-3 docks at the vacuole membrane to release its cargoes (Fig. 1A, right) (32). There are links between the AP-3 complex and polyP storage in higher eukaryotes. In humans, mutations in AP-3 are associated with a rare disorder called Hermansky-Pudlak syndrome (33–35). Hermansky-Pudlak syndrome patients lack the ability to synthesize lysosome-related organelles in diverse cell types throughout the body, which results in broad

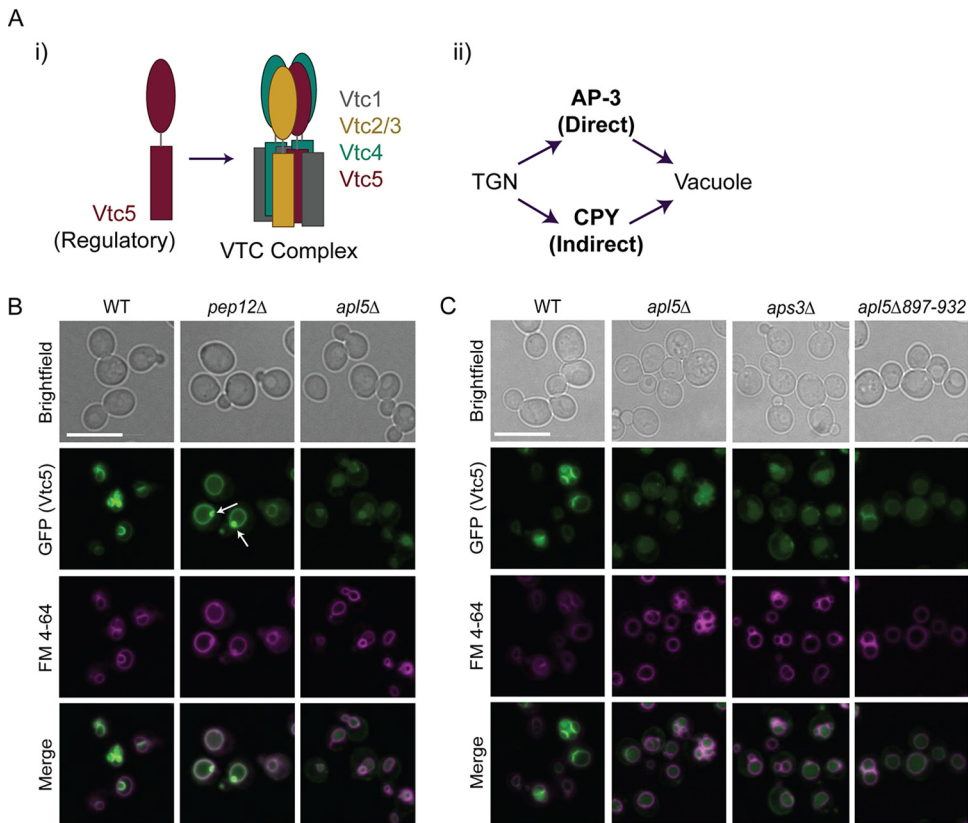


FIG 1 GFP-Vtc5 is localized to the vacuole membrane via the conserved AP-3 pathway. (A) Schematic of the proposed VTC complex subunit organization (i) and a simplified schematic of protein transport to the vacuole in *S. cerevisiae* (ii). Organization of the VTC complex was proposed by Gerasimaitė et al. (9). (B) The indicated strains were grown in YPD prior to incubation with FM 4-64, which marks the vacuole membrane, for 2 h. Cells were then washed with fresh YPD for 30 min, transferred to synthetic medium, and imaged. Live-cell fluorescence microscopy was performed using a Leica DMI 6000 microscope at 63 \times with oil immersion. For AP-3 mutants, green (GFP-Vtc5) images were taken at longer exposure times to account for differences in signal intensity. Images were processed in Fiji. Bar, 10 μ m. Puncta are indicated by white arrows. (C) The indicated strains were processed as described for panel B. Maximum intensities for individual panels are adjusted to account for variations in intensity of original images. Also see Fig. S1 to S3.

phenotypes that include albinism, visual impairment, and bleeding problems (35). Notably, this includes the inability to generate dense granules in platelets, where polyP is usually stored in its highest concentrations (130 mM) (36). PolyP promotes blood clotting by acting on proteins involved in the coagulation cascade, including factor XII (37), factor XI (38), factor V (39), and thrombin (40). PolyP addition re-establishes clotting stimulatory activity of platelets derived from Hermansky-Pudlak syndrome patients (41).

In this study, we describe a role for the yeast AP-3 complex in localizing Vtc5 to the vacuole membrane. In AP-3 mutants, Vtc5 is rerouted to the vacuole lumen by the endosomal sorting complex required for transport (ESCRT), where it is degraded by the vacuolar protease Pep4. Mislocalization of Vtc5 in AP-3 mutants is accompanied by a decrease in VTC protein levels and decreased levels of polyP. Overall, our study explains the polyP accumulation defects in AP-3 mutants and provides novel insights into the regulation of the VTC polyP synthetase in budding yeast.

RESULTS

Vtc5 localization to the vacuole membrane is disrupted in AP-3 mutants. The CPY and AP-3 pathways constitute the two major routes of protein transport to the vacuole from the TGN (Fig. 1A). To test which of these pathways is responsible for Vtc5 localization to the vacuole membrane, we used live-cell fluorescence microscopy to

analyze green fluorescent protein (GFP)-Vtc5 localization in AP-3 and CPY pathway mutants. Notably, all N-terminal GFP-Vtc fusions used in this work are functional, with the GFP tag facing the cytoplasmic side of the vacuole membrane to ensure that the tag is not degraded within the vacuole lumen (12, 22). These GFP fusions are expressed from constitutive promoters integrated at endogenous *VTC* loci (see Materials and Methods). In wild-type cells, GFP-Vtc5 (green) localized exclusively to the vacuole membrane, as demonstrated by colocalization with FM 4-64 (magenta), a dye which labels the vacuole membrane (Fig. 1B). CPY mutants (*pep12Δ*) also showed GFP-Vtc5 accumulation on the vacuole membrane, but this localization was accompanied by the appearance of puncta at the surface of some vacuoles (Fig. 1B). These puncta may signify partially defective transport through this pathway (42). In contrast, GFP-Vtc5 was clearly mislocalized to the vacuole lumen in AP-3 mutant (*apl5Δ*) cells (Fig. 1B). AP-3 is highly conserved from yeast to humans. It consists of a heterotetramer of four protein subunits: two large subunits (Apl6/AP3β1 and Apl5/AP3δ1), one medium subunit (Apm3/AP3μ1), and one small subunit (Aps3/AP3σ1) (see Fig. S1A in the supplemental material) (43). Deletion of genes encoding any one of the four AP-3 subunits results in defects in AP-3 cargo transport (44). Therefore, to corroborate our results with *apl5Δ*, we examined GFP-Vtc5 localization in *aps3Δ* cells and again observed its mislocalization to the vacuole lumen in this mutant (Fig. 1C). While the presence of GFP-Vtc5 on the vacuole membrane appears to depend on AP-3, we cannot rule out the possibility that the CPY pathway may also contribute to its delivery under some circumstances.

Intriguingly, polyP chains can be covalently attached to protein targets as a post-translational modification termed polyphosphorylation (27, 45). Polyphosphorylation is the nonenzymatic addition of polyP chains onto lysine residues, principally within poly-acidic, serine, and lysine (PASK)-rich clusters (27, 46). We previously reported that Apl5 is polyphosphorylated in its C-terminal PASK cluster (amino acids 897 to 932) (47). Therefore, to test if polyphosphorylation impacts Apl5's role in localizing GFP-Vtc5 to the vacuole membrane, we first deleted the PASK cluster in its entirety. Deletion of Apl5's PASK cluster (*apl5Δ897-932*) resulted in mislocalization of GFP-Vtc5 to the vacuole lumen, similar to what we observed in AP-3-null mutants (Fig. 1C). To define the contribution of polyphosphorylation more specifically, we generated a strain wherein endogenous Apl5 is expressed with 13 lysine-to-arginine (K-R) amino acid substitutions in its PASK cluster. Polyphosphorylation results in an electrophoretic shift of target proteins separated on bis-Tris NuPAGE gels (27, 48), and this is currently the only method described for evaluation of this new modification. As demonstrated by NuPAGE analysis, the resulting mutant (Apl5_{PASK}K-R) was unable to undergo polyphosphorylation (Fig. S1B). However, this did not impact GFP-Vtc5 localization (Fig. S1C), nor did it mimic other known *apl5Δ* phenotypes, such as defects in the maturation of AP-3 target Pho8, a vacuolar alkaline phosphatase (49) (Fig. S1D), or enhanced sensitivity to nickel chloride (50) or rapamycin (51) (Fig. S2A and B). We note that the PASK cluster lies within Apl5's Vps41 binding domain (52). Vps41 is a member of the homo-typic fusion and protein sorting (HOPS) complex required for vesicle docking at the vacuole and delivery of AP-3 cargoes (52, 53). As such, the role of the Apl5 PASK in GFP-Vtc5 delivery may stem from disruption of this interaction rather than a defect in polyphosphorylation. Interestingly, the Apl5 C-terminal PASK deletion mutant (*apl5Δ897-932*) showed defects in maturation of Pho8, but it did not result in sensitivity to nickel chloride or rapamycin (Fig. S1D and S2A and B). This separation-of-function mutant may serve as a useful tool to dissect AP-3's role underlying these distinct phenotypes.

We next sought to test whether vacuolar localization of additional VTC subunits was also impacted by *APL5* deletion. We observed no concrete difference in the localization of GFP-Vtc3 in wild-type cells versus *apl5Δ* mutants (Fig. S3A). GFP-Vtc4 showed an intermediate phenotype, with increased localization to the cytoplasm in *apl5Δ*, with some protein also remaining at the vacuole membrane (Fig. S3B). These data suggest

that although the AP-3 pathway is responsible for the proper vacuolar localization of GFP-Vtc5, other pathways may contribute to the localization of core VTC subunits. Given the importance of Vtc5 as a regulator of VTC activity and the clear disruption of its localization in AP-3 mutants, we focused on the transport of this subunit.

GFP-Vtc subunits are degraded in cells lacking functional AP-3. We next used Western blotting to gain insight into the fate of mislocalized GFP-Vtc5. Relative to wild-type controls, *apl5Δ* and *aps3Δ* cells showed a striking accumulation of free GFP, which is known to be resistant to degradation (Fig. 2A and B) (54). This was not the result of increased protein expression, as full-length GFP-Vtc5 was reduced in these mutants (Fig. 2A and C). This pattern was observed previously for other proteins mislocalized to the vacuole lumen and is attributed to cargo degradation (55, 56). We also tested if GFP-Vtc4 and GFP-Vtc3 levels were similarly affected. Both GFP-Vtc4 and GFP-Vtc3 also accumulated free GFP at the expense of decreased full-length fusions, although the effect was not as dramatic as that observed for GFP-Vtc5 (Fig. 2D to I). Previous work from the Mayer group showed that *vtc5Δ* cells have decreased levels of core VTC subunits at the vacuole membrane (22). Degradation of GFP-Vtc3 and GFP-Vtc4 and partial mislocalization of GFP-Vtc4 in *apl5Δ* cells are consistent with a model wherein mislocalized Vtc5 is largely nonfunctional in the absence of AP-3. However, we cannot exclude the possibility that these molecular phenotypes stem in part from defects in the transport of other AP-3 cargoes (see Discussion).

Mislocalized Vtc5 is rerouted to the vacuole lumen by the ESCRT pathway. We next investigated which pathways are responsible for localizing GFP-Vtc5 to the vacuole lumen in the absence of functional AP-3, with a focus on the autophagy and ESCRT pathways. Autophagy is a process whereby cytoplasmic material becomes sequestered in vesicles that fuse to the vacuole to deliver their contents for degradation (57). The ESCRT pathway is responsible for detecting ubiquitylated transmembrane proteins to sort them into multivesicular bodies (MVBs) in the endocytic pathway for delivery to the vacuole (58). Disruption of ESCRT (*vps27Δ*) but not autophagy (*atg8Δ*) in AP-3 mutants resulted in a loss of GFP signal from the vacuole lumen (Fig. 3A). In contrast, neither pathway impacted GFP-Vtc5 localization in wild-type cells (Fig. S4A). When ESCRT subunits are mutated, the complex becomes defective for proper MVB biogenesis and fusion at the vacuole membrane (58). Indeed, in *apl5Δ vps27Δ* double mutants, GFP-Vtc5 appeared to accumulate in FM 4-64-labeled vesicles around the vacuole membrane (Fig. 3A). Deletion of *VPS27* also resulted in reversal of free GFP accumulation in Western blots (Fig. 3B). The same molecular phenotype was observed across multiple ESCRT mutants (ESCRT-0, -I, -II, and -III) (Fig. S4B).

The ESCRT pathway recognizes cargoes that have been ubiquitylated by E3 ubiquitin ligases (58, 59). These cargoes are then transported to the vacuole via MVBs that fuse with the vacuole membrane. As one of the last steps in this process, the deubiquitinase Doa4 removes and recycles ubiquitin moieties from ESCRT-targeted proteins upon cargo delivery to the vacuole (58, 59). Mutation of *DOA4* alone had no impact on GFP-Vtc5 processing or localization (Fig. 3C and Fig. S4C). In AP-3 mutants, however, *doa4Δ* prevented the accumulation free GFP, mirroring what was observed for ESCRT mutants (Fig. 3C). Moreover, *doa4Δ* also restored robust GFP-Vtc5 localization to the vacuole membrane (Fig. 3D). Taking these results together, we conclude that Doa4 is a key player in localizing Vtc5 to the vacuole lumen in the absence of AP-3. Finally, when proteins accumulate in the lumen, they become accessible to vacuole proteases (60). Deletion of the major vacuolar protease Pep4 reversed the accumulation of free GFP in AP-3 mutants (Fig. 3B), without impacting total GFP accumulation in the vacuole lumen (Fig. 3A), suggesting that Pep4 is a major protease responsible for GFP-Vtc5 degradation.

The AP-3 complex is required for maintenance of wild-type polyP levels. Finally, we tested the contribution of AP-3 to polyP homeostasis. Deletion of AP-3 subunits resulted in a clear decrease in polyP levels (Fig. 4A). This finding is consistent with previous data wherein AP-3 mutants were found to be important for polyP accumulation in a large-scale screen (61). We observed a similar result in our strains used for prior

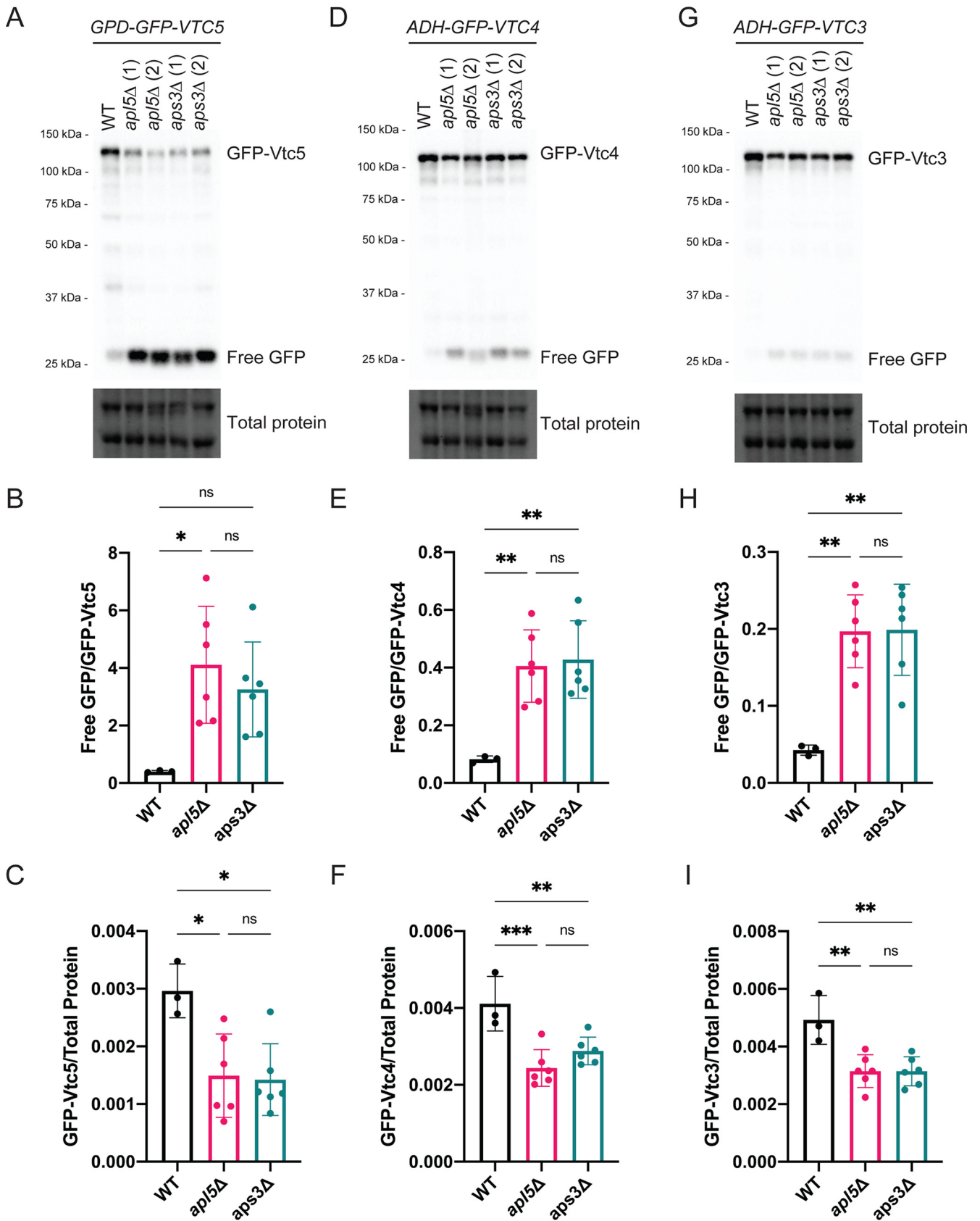


FIG 2 AP-3 mutation causes degradation of GFP-Vtc proteins. (A) Upon AP-3 mutation (*apl5Δ* and *aps3Δ*), full-length GFP-Vtc5 protein levels are reduced with a concomitant increase in free GFP. Proteins were extracted from the indicated strains using a TCA protein extraction protocol, separated on a 10% (Continued on next page)

analyses where GFP-Vtc5 is expressed under the control of a constitutive *GPD1* promoter (Fig. 4B). Together with our previous results, these data suggest that correct localization of Vtc5 to the vacuole membrane by the AP-3 complex is important for its function. Notably, AP-3 mutants still have more polyP than cells lacking Vtc5 altogether (*vtc5Δ*) (Fig. 4C). This observation could be explained by residual localization of Vtc5 to the vacuole membrane in AP-3 mutants. We note that the decrease in polyP observed in *apl5Δ* mutants is largely epistatic with *vtc5Δ*, consistent with the notion that they function within the same pathway (Fig. 4C). Interestingly, deletion of *DOA4*, which rescues GFP-Vtc5 processing and localization to the vacuole membrane, was unable to reverse the decreased polyP levels in *apl5Δ* mutants (Fig. 4D). Thus, proper function of GFP-Vtc5 requires localization to the vacuole membrane, specifically through the AP-3 pathway.

DISCUSSION

AP-3 regulation of Vtc5 localization. Interest in polyP research has experienced a resurgence in recent years on the heels of the discovery of exciting connections between polyP and diverse aspects of cell signaling and protein homeostasis. With the key players involved in mammalian polyP metabolism largely uncharacterized, model systems have proved essential to our understanding of polyP dynamics and function. In *S. cerevisiae*, polyP is synthesized by the vacuole-bound VTC complex and stored at high concentrations in the vacuole (13). The activity of the core VTC complex (consisting of Vtc1, Vtc2 or Vtc3, and Vtc4) is increased dramatically by the Vtc5 subunit (22). This is the only protein known to act directly on the VTC complex to stimulate polyP production. Our study supports a model where Vtc5 localization to the vacuole membrane depends on the evolutionarily conserved AP-3 complex. This finding provides insight into the regulation of the VTC complex and identifies Vtc5 as a cargo whose mislocalization underlies polyP accumulation defects observed in AP-3 mutants.

We propose that in wild-type cells (Fig. 5), Vtc5 is sorted into AP-3-coated vesicles at the TGN and transported directly to the vacuole. The AP-3 complex selects protein cargoes by tyrosine-based motifs (YXXØ, where X represents any amino acid and Ø is a bulky hydrophobic amino acid) and/or dileucine-based motifs ([D/E]XXXL[L/I], where X represents any amino acid) (62). Notably, Vtc5 has 6 tyrosine-based motifs and 2 dileucine-based motifs, which together could be used as a targeting signal. Alternatively, Vtc5 could be transported in conjunction with other AP-3 cargoes, such as Vam3, which is also required for wild-type levels of polyP accumulation (61). Regardless, it is likely that Vtc5 delivery requires interaction of AP-3 coated vesicles with Vps41 of the HOPS complex, which facilitates docking and release of cargo into the vacuole membrane (52, 63–65). In the absence of AP-3, Vtc5 is mislocalized to the vacuole lumen. Mislocalized Vtc5 (e.g., in *apl5Δ*), is recognized and sorted by the ESCRT pathway into the vacuole lumen via the endosomal system, where it is eventually degraded in a manner dependent on vacuolar protease Pep4 (Fig. 5). Since Pep4 is also required for the activation of vacuolar proteases Prb1 and Prc1 (66, 67), it is possible that these also play a role in Vtc5 degradation in the vacuole lumen.

We found that degradation of Vtc5 in AP-3 mutants requires the Doa4 deubiquitinase. *DOA4* is required for sorting of many ESCRT-dependent cargoes into the endosomal system (68), and *doa4Δ* mutants have decreased levels of free ubiquitin (69). Therefore, it is very likely that mislocalized Vtc5 is subject to regulation by ubiquitylation. Indeed, several large-scale studies have identified ubiquitylation sites in the

FIG 2 Legend (Continued)

Bio-Rad TGX Stain-Free FastCast acrylamide gel, and transferred to a nitrocellulose membrane. The membrane was imaged on a Bio-Rad ChemiDoc system after immunoblotting with anti-GFP. Total protein was imaged as a loading control. (B and C) Quantification of free-GFP/GFP-Vtc5 ratios and full-length GFP-Vtc5 levels. Quantifications were done using Bio-Rad ImageLab software, and graphs were created using Prism GraphPad software. One-way ANOVA were performed with Tukey *post hoc* tests. *, $P < 0.05$; **, $P < 0.01$; ***, $P < 0.001$; ns, not significant. Error bars represent standard deviations of the mean. $n = 3$ for the wild type (WT) and $n = 6$ for AP-3 mutants. (D to F) In AP-3 mutants, GFP-Vtc4-expressing strains accumulate free GFP at the expense of full-length protein. The methods were the same as for panels A to C. (G to I) In AP-3 mutants, GFP-Vtc3-expressing strains accumulate free GFP at the expense of full-length protein. The methods were the same as for panels A to C.

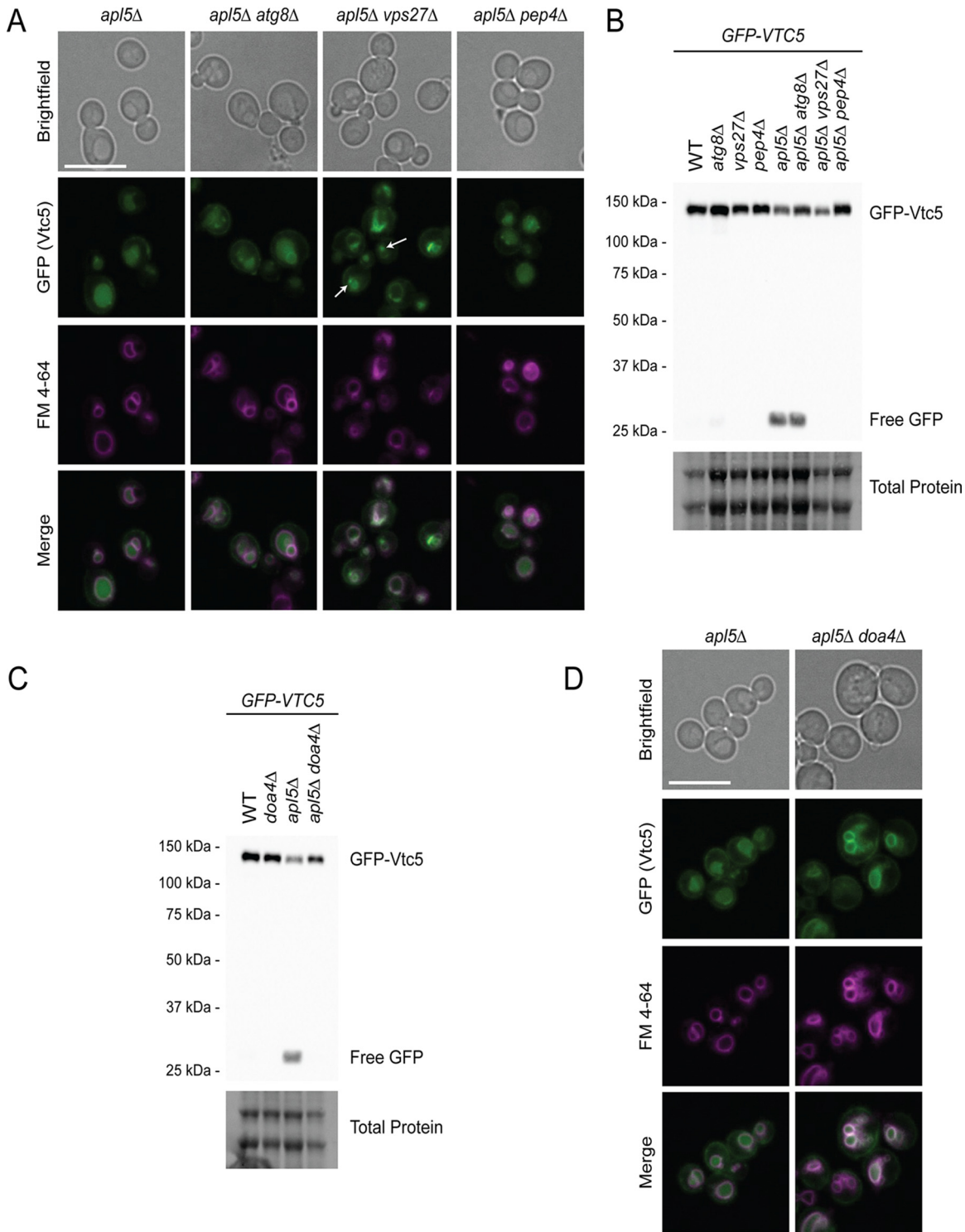


FIG 3 Degradation of mislocalized GFP-Vtc5 depends on ESCRT and the Pep4 protease. (A) The mislocalization of GFP-Vtc5 upon AP-3 mutation is mediated by the ESCRT pathway. Cells were grown in YPD prior to incubation with FM4-64, which marks the vacuole membrane, for 2 h. Cells were then washed with fresh YPD for 30 min, transferred to synthetic medium, and imaged. Live-cell fluorescence microscopy was performed using a Leica DMI 6000 at 63 \times with oil immersion. Images were processed in Fiji. Bar, 10 μ m. White arrows indicate potential MVBs at the vacuole. For *apl5Δ* and *apl5Δ atg8Δ* strains, maximum intensities for the FM 4-64 channel were set lower than for other strains to accommodate differences in FM 4-64 staining. (B) Free GFP accumulation in GFP-Vtc5 strains, mediated by AP-3 mutation, is reversed by ESCRT (*vps27Δ*) and *pep4Δ* mutation. Proteins from the indicated strains were extracted using a TCA protein extraction protocol, separated on a 10% Bio-Rad TGX Stain-Free FastCast acrylamide gel, and transferred to a nitrocellulose membrane. The membrane was imaged for total protein and probed using an anti-GFP antibody to detect GFP-Vtc5 protein using a Bio-Rad ChemiDoc. (C) GFP-Vtc5 degradation and free GFP accumulation is reversed by *DOA4* deletion. The method was the same as for panel B. (D) Deletion of *DOA4* rescues localization of GFP-Vtc5 in *apl5Δ* mutants. The method was the same as for panel A. Also see Fig. S4.

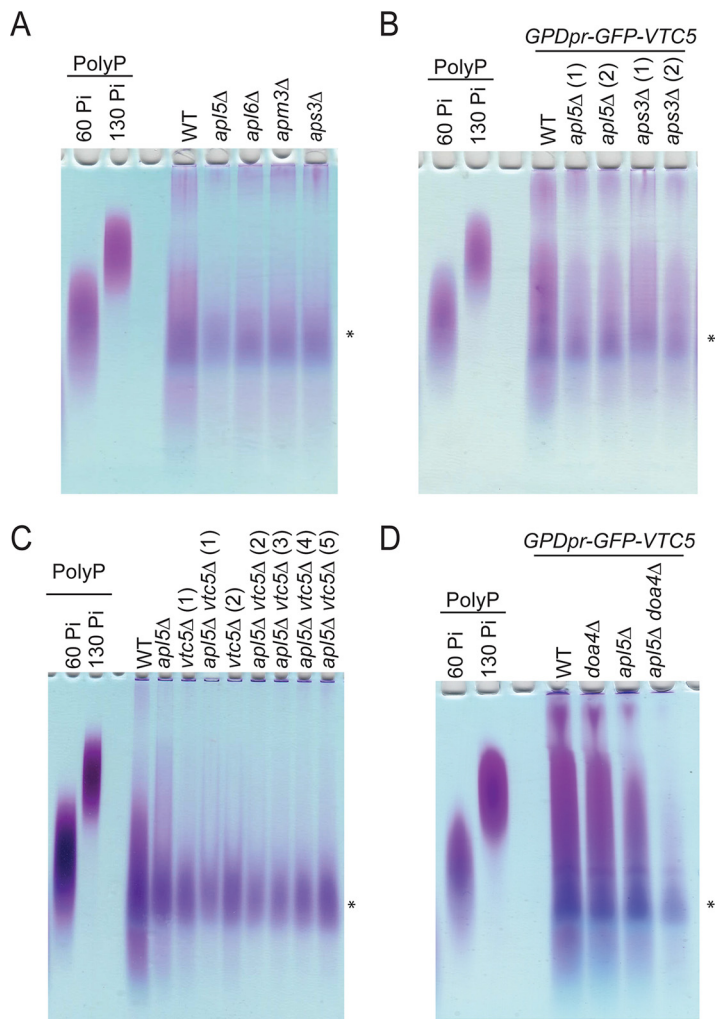


FIG 4 Functional AP-3 is required for the maintenance of polyP levels. (A) An AP-3 subunit mutant causes a reduction in polyP levels. There is a loss of polyP when each of the four AP-3 subunits (*apl5Δ*, *apl6Δ*, *apm3Δ*, and *aps3Δ*) is mutated. PolyP was extracted as described in Materials and Methods. After extraction, samples were mixed with polyP loading dye and separated on a 15.8% TBE-urea acrylamide gel. The gel was incubated in fixing solution with toluidine blue for 15 min prior to destaining and imaging. PolyP with chain lengths of 60 and 130 P_i units are included as standards. (B) AP-3 mutants (*apl5Δ* and *aps3Δ*) cause a reduction in polyP levels when GFP-Vtc5 is expressed under the control of a *GPD1* promoter. The method was the same as for panel A. (C) Mutating AP-3 (*apl5Δ*) and *vtc5Δ* results in a largely epistatic decrease in polyP levels. The method was the same as for panel A. (D) Although *doa4Δ* is capable of rescuing GFP-Vtc5 localization and protein degradation when AP-3 is mutated (Fig. 3C and D), it is incapable of restoring polyP levels. The method was the same as for panel A. The asterisks indicate a background contaminant in extractions. Numbers indicate independent strains.

middle and C-terminal regions of the protein (70). We speculate that these sites may be targets of the Rsp5 E3 ubiquitin ligase, which has been implicated in the ESCRT-dependent delivery of proteins to the vacuole lumen (71–73). Notably, Vtc5 is also rich in phosphoserines, including those potentially regulated by the Cdk1 (cell cycle) and Nnk1 (nitrogen metabolism) kinases (70). These modifications could impact Vtc5 localization in wild-type or AP-3 mutant cells or may instead be involved in regulating its activity toward the core VTC complex.

Regulation of the core VTC complex. In contrast to GFP-Vtc5, we found that localization of GFP-Vtc3 to the vacuole membrane was not impacted by disruption of AP-3 and GFP-Vtc4 was only partially affected. However, deletion of AP-3 subunits still reduced GFP-Vtc3/4 protein levels and the increased appearance of free GFP in

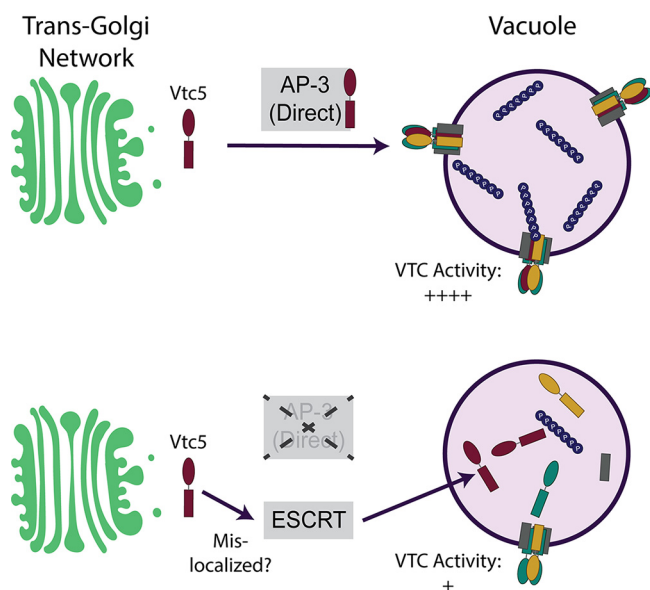


FIG 5 GFP-Vtc5 is localized to the vacuole membrane via the AP-3 complex. In the absence of AP-3, mislocalized GFP-Vtc5 could be localized at the plasma membrane or elsewhere in the cell prior to recognition by ESCRT and delivery to the vacuole lumen for Pep4-dependent degradation. However, we cannot rule out the possibility that Vtc5 is incorrectly inserted at the vacuole membrane prior to ESCRT-dependent internalization. See the text for details.

Western blots, albeit to a lesser degree than that observed for GFP-Vtc5. We suggest that transport of core VTC subunits occurs through multiple transport routes, although these may function redundantly with AP-3. This type of dual regulation has been documented for other AP-3 cargoes, such as Sna4 (56) and Ypq1 (74). It is also possible that changes observed in core subunits stem from mislocalized Vtc5. There is strong evidence that maximal polyP production requires VTC localization to the vacuole (13). However, polyP has also been detected in variable amounts at the plasma membrane, cytoplasm, mitochondria, and nucleus (14). Whether vacuolar polyP is somehow transported to these compartments or whether it is made by VTC residing locally remains an open question. In the latter case, it is possible that a lack of Vtc5 colocalization with core VTC subunits in these areas ensures that subcellular concentrations of polyP outside the vacuole are kept low. However, it is not clear if Vtc5 localization may change throughout the cell cycle or in response to specific stresses, and this remains an important area for future work. It will also be intriguing to identify pathways that regulate localization of GFP-Vtc2, which is found at the plasma membrane or peripheral endoplasmic reticulum under phosphate-replete conditions, becoming enriched at the vacuole only under conditions of phosphate starvation (9, 12, 15).

AP-3 impact on polyP levels. Our work shows that AP-3 mutant cells have reduced levels of polyP. This was true both in a wild-type background and under conditions of Vtc5 overexpression. These findings are consistent with work from Freimoser et al. identifying AP-3-encoding genes in a genome-wide screen for deletion mutations with defects in polyP accumulation (61). Interestingly, deletion of *DOA4* in an AP-3 mutant background rescued both GFP-Vtc5's localization to the vacuole membrane and GFP-Vtc5 degradation without restoring polyP levels. In fact, polyP levels in *apl5Δ doa4Δ* double mutants were lower than in either single mutant. While this may seem counterintuitive, we suggest that Vtc5 is not correctly positioned within the vacuole membrane under these circumstances and is unable to stimulate VTC activity. The reduction in polyP levels seen in AP-3 mutants is not as dramatic as that observed in cells lacking Vtc5 altogether, suggesting either that there is residual localization of Vtc5 to the vacuole membrane or that mislocalized Vtc5 remains competent to stimulate core VTC activity to some degree. Notably, Freimoser et al. identified over 200 additional genes

that impact polyP metabolism (61), and some of these could function as direct regulators of Vtc5 or AP-3.

We recently described the Apl5 subunit of AP-3 as a target of lysine polyphosphorylation (47). However, our analysis of mutant Apl5 that cannot be polyphosphorylated suggests that this modification does not impact GFP-Vtc5 delivery to the vacuole or other AP-3 related phenotypes that we tested. Polyphosphorylation of AP-3 may become important under selected stress conditions that remain to be identified. Since polyP has been described as having chaperone activity (4), another possibility is that polyphosphorylation promotes degradation or refolding of a small fraction of AP-3 that is itself mislocalized to the polyP-rich vacuole lumen.

Conservation of the AP-3 complex and function. The AP-3 complex is highly conserved in mammalian cells in terms of subunit organization and function. For example, the human homolog of Ypq1, PQLC2, is transported to the vacuole membrane by the AP-3 complex when it is expressed in yeast (74). Notably, mutations in human AP-3 give rise to Hermansky-Pudlak syndrome. Relevant here is the observation that molecular phenotypes of Hermansky-Pudlak syndrome patients include a failure to accumulate polyP in platelet dense granules, a type of lysosome-related organelle conceptually similar to the yeast vacuole (33–35). Based on the conserved role of AP-3 subunits in polyP metabolism, we suggest that identification and characterization of AP-3 cargoes in human cells that accumulate high levels of polyP may provide unique insights into the human polyP synthetases, the identity of which remains a critical open question in the field.

MATERIALS AND METHODS

Yeast strains and handling. Yeast strains were constructed using standard techniques via transformation of PCR products containing selectable markers. For gene deletions, PCR analyses were used to confirm the position of the gene deletion and the absence of a wild-type gene copy. PCR was also used to confirm the correct genomic location of cassettes used for epitope tagging. Genotypes for all strains used in this study are listed in the supplemental tables. For all experiments performed strains were grown in yeast extract-peptone-dextrose (YPD; 2% glucose supplemented with 0.005% adenine and 0.005% tryptophan).

Apl5 K-R mutagenesis. A construct containing the lysine (K)-to-arginine (R) mutations within Apl5 PASK cluster was custom created by GenScript and used for the experiments listed in Fig. S1 and S2. The construct was integrated with a GFP tag or FLAG tag at the endogenous *APL5* locus using transformation of overlapping PCR products.

Electrophoresis and immunoblotting. Methods for protein extraction were described previously (48) and are summarized here using similar wording for clarity. A BioSpec bead beater was used to lyse cell pellets corresponding to 3 to 6 units of optical density at 600 nm (OD_{600}) in the presence of 100 μ l of acid-washed beads and 300 μ l of 20% trichloroacetic acid (TCA) (Sigma-Aldrich T6399). Two 3-min pulses were used. The supernatant was recovered, and cells were washed with 300 μ l of 5% TCA (Sigma-Aldrich T6399). The supernatant from the second wash was combined with the first, and this mixture was clarified by centrifugation at 4°C at 16,000 $\times g$ for 4 min. The supernatant was removed, and the pellet was resuspended in SDS-PAGE sample buffer (see buffer recipes below) supplemented with 1/10 volume of 1.5 M Tris-HCl, pH 8.8 (Tris base [Fisher BP152-5], hydrochloric acid [Fisher A144-212]), and 1/10 volume 1 M dithiothreitol (DTT) (Bio Basic DB0058). Samples were boiled for 5 min before an additional centrifugation at 4°C at 16,000 $\times g$ for 4 min. The supernatant was recovered and stored or used immediately for SDS-PAGE or NuPAGE analysis (Thermo Fisher NP0336). Where indicated, Bio-Rad TGX Stain-Free FastCast 10% acrylamide (Bio-Rad 1610183) was used for quantification, with total protein quantified in place of a loading control. Bio-Rad TGX acrylamide gels were transferred to nitrocellulose membranes (Bio-Rad 162-0112), and exposures were obtained using a Bio-Rad ChemiDoc system. Non-TGX 12% SDS-PAGE and NuPAGE gels (Thermo Fisher NP0336) were transferred to polyvinylidene difluoride (PVDF) membranes (Bio-Rad 162-0177), and exposures were obtained using autoradiography film (Harvard Apparatus Canada DV-E3018). In all cases, Luminata Forte enhanced chemiluminescence (ECL) (Fisher Scientific WBLUF0500) was employed for detection. All antibodies used for immunoblotting are described in the supplemental tables.

Spot tests. Cells were diluted to an OD_{600} of 0.1, grown for 4 h, and then diluted again to an OD_{600} of 0.1 prior to being serially diluted 5-fold in H₂O. Four microliters of each dilution was spotted on the indicated medium prior to incubation at 30°C for 2 to 3 days. Plates contained the following chemicals/drugs: 0.028% dimethyl sulfoxide (DMSO) (VWR CA97061-250), 0.75 mM NiCl₂ (Fisher N54-250), and 0.003 μ M rapamycin (Sigma-Aldrich R0395-1MG). Images were taken using a Bio-Rad ChemiDoc system.

Microscopy. Live-cell fluorescence imaging was conducted using a Leica DMI 6000 microscope with a Hamamatsu camera using the Volocity 4.3.2 imaging program. Briefly, cells were diluted to an OD_{600} of 0.2 from overnight cultures in YPD. After 3 h of growth at 30°C, FM 4-64 (Thermo Fisher T13320; 1.64 mM stock in DMSO) was added to a final concentration of 1.64 μ M for an additional 2 h. Cells were

then washed out in YPD for 30 min at room temperature. In instances where there was a difference in protein expression level, exposure times were taken at longer intervals to account for this discrepancy (e.g., Fig. 1). For microscopy whose results are shown in Fig. S3, images were taken on a Zeiss AxioObserver 7 microscope with a Hamamatsu ORCA-Flash LT camera using Zeiss Zen 3.0 Pro Software. All images were taken with oil immersion at 63 \times . All images were then analyzed in FIJI. Backgrounds were subtracted with a rolling-ball radius of 50 pixels, and images taken with FM 4-64 dye were converted from red to magenta. For microscopy images, Mix/Max values in FIJI were chosen to highlight representative changes in subcellular localization across multiple fields of view.

Polyphosphate extractions. Polyphosphate was extracted from yeast pellets containing 8 to 12 OD₆₀₀ units using an adapted protocol from Bru et al. (7, 75). Cells were resuspended in 400 μ l of cold LETS buffer (see buffer recipes below). Subsequently, 600 μ l of neutral phenol pH 8 (Sigma-Aldrich P4557) and 150 μ l of Milli-Q H₂O were added. Samples were vortexed for 20 s and heated for 5 min at 65°C followed by a 1-min incubation on ice. Six hundred microliters of chloroform (Sigma-Aldrich 472476) was added, and samples were vortexed for 20 s and spun down at room temperature for 2 min at 13,000 \times g. The top layer was then transferred to a new tube containing 600 μ l of chloroform (Sigma-Aldrich 472476), vortexed for 20 s and spun down at room temperature for 2 min at 13,000 \times g. The top layer was transferred to a new tube and 2 μ l of RNase A (10 mg/ml; Thermo Fisher R1253) and 2 μ l of DNase I (10 mg/ml; Thermo Fisher AM2222) were added, followed by a 1-h incubation at 37°C. The mixture was transferred to a prechilled tube containing 1 ml 100% ethanol (Commercial Alcohols P006EAA) and 40 μ l of 3 M sodium acetate, pH 5.3 (Sigma-Aldrich S7899). Samples were left at -20°C overnight and then centrifuged for 20 min at 13,000 \times g at 4°C. The pellet was washed in 500 μ l of cold 70% ethanol (Commercial Alcohols P006EAA) and centrifuged for 5 min at 13,000 \times g at 4°C. The supernatant was discarded, and the pellet was air dried before resuspension in 20 to 30 μ l mlH₂O. Samples were mixed 1:1 with polyP loading dye (see buffer recipes below) and electrophoresed on a 15.8% Tris-borate-EDTA (TBE)-urea acrylamide gel at 100 V for 1 h and 45 min in 1 \times TBE buffer (see buffer recipes below). The gel was incubated in fixing solution (see buffer recipes below) with toluidine blue for 15 min and then destained in destaining solution. PolyP standards (a gift from T. Shiba) were used to assess polyP chain length.

Statistical analyses. For statistical analyses performed on Western blots in Fig. 2, a one-way analysis of variance (ANOVA) was performed with Tukey *post hoc* tests at 95% confidence intervals. Error bars, *P* values, and numbers of biological replicates (*n*) are defined in the relevant figure legends.

Buffer recipes. The following buffer recipes are taken from our previous study (48) and are listed here for convenience.

SDS-PAGE running buffer (1 \times working concentration) consists of 100 ml of 10 \times 1 liter stock (30.2 g Tris base [Fisher BP152-5], 188 g glycine [Fisher BP381-5], 10 g SDS [Fisher BP166]) and 900 ml double-distilled water (ddH₂O). Note that SDS-PAGE gels do not resolve polyP shifts.

NuPAGE running buffer (1 \times working concentration) consists of 50 ml of 20 \times 1 liter stock (209.2 g MOPS [Sigma M1254], 121.1 g bis-Tris [Sigma B9754], 20 g SDS [Fisher BP166], 12 g EDTA [Sigma ED255]), 5 ml of 1 M sodium bisulfite (Fisher S654-500), and 950 ml ddH₂O.

SDS-PAGE transfer buffer (1 \times working concentration) consists of 100 ml of 10 \times 1 liter stock (30.275 g Tris base [Fisher BP152-5], 166.175 glycine [BioBasic GB0235]), 200 ml methanol (Fisher A412P-4), and 700 ml ddH₂O.

NuPAGE transfer buffer (1 \times working concentration) consists of 50 ml of 20 \times 1 liter stock (81.6 g Bicine [Sigma B3876], 104.8 g bis-Tris [Sigma B9754], 6 g EDTA [Sigma ED255]), 200 ml methanol (Fisher A412P-4), and 750 ml ddH₂O.

SDS-PAGE/NuPAGE sample buffer (3 \times stock) consists of 800 μ l of stock (160 mM Tris-HCl [pH 6.8] [Tris base [Fisher BP152-5], hydrochloric acid [Fisher A144-212]], 6% SDS [wt/vol] [Fisher BP166], 30% glycerol [Fisher BP229-4], 0.004% bromophenol blue [Fisher BP115-25]). For TCA preparations, 3 \times is supplemented with 100 μ l 1 M DTT (BioBasic DB0058) and 100 μ l 1.5 M Tris-HCl (pH 8.8) (Tris base [Fisher BP152-5], hydrochloric acid [Fisher A144-212]).

The following buffer recipes are from this current study.

TBE (1 \times working concentration) consists of 200 ml of a 5 \times stock (67.5 g Tris base [Fisher BP152-5], 34.37 g boric acid [Fisher BP168-1], and 25 ml 0.5 M EDTA [Sigma-Aldrich 03690]) and 800 ml ddH₂O.

LETS buffer (1 \times working concentration) consists of 100 mM LiCl (Fisher L120-500), 10 mM EDTA (Sigma-Aldrich 03690), 10 mM Tris-HCl (pH 7.4) (Tris base [Fisher BP152-5], hydrochloric acid [Fisher A144-212]), and 20% SDS (Thermo Fisher AM9820).

PolyP loading dye (6 \times) consists of 10 mM Tris-HCl (pH 7) (Tris base [Fisher BP152-5], hydrochloric acid [Fisher A144-212]), 1 mM EDTA (Sigma-Aldrich 03690), 30% glycerol (Fisher BP229-4), and bromophenol blue (Fisher BP115-25).

Toluidine blue fixing solution consists of 25% methanol (Fisher A412P), 5% glycerol (Fisher BP229-4), and 0.05% toluidine blue (Sigma-Aldrich T3260).

Destaining solution consists of 25% methanol (Fisher A412P) and 5% glycerol (Fisher BP229-4).

SUPPLEMENTAL MATERIAL

Supplemental material is available online only.

FIG S1, TIF file, 2.3 MB.

FIG S2, TIF file, 2.2 MB.

FIG S3, TIF file, 2.3 MB.

FIG S4, TIF file, 2.7 MB.

TABLE S1, XLSX file, 0.01 MB.

TABLE S2, XLSX file, 0.01 MB.

ACKNOWLEDGMENTS

We thank A. Mayer for yeast strains, T. Shiba (Regentiss, Japan) for polyP standards, and members of the Downey lab for critical reading of the manuscript. We thank Alix Denoncourt for help with polyP extractions. We also acknowledge the Cell Biology and Image Acquisition Core, funded by the University of Ottawa and the Canada Foundation for Innovation, for microscopy training and expertise.

Work for this project was funded by a Canadian Institutes of Health Research (CIHR) Project Grant (PJT-148722), and by an Early Researcher Award from the Ontario Ministry of Innovation and Research to M.D. A.B.-D. was funded in part by a graduate scholarship from the Natural Sciences and Engineering Research Council of Canada (NSERC).

We declare no conflicts.

REFERENCES

- Rao NN, Gomez-Garcia MR, Kornberg A. 2009. Inorganic polyphosphate: essential for growth and survival. *Annu Rev Biochem* 78:605–647. <https://doi.org/10.1146/annurev.biochem.77.083007.093039>.
- Roewe J, Stavrides G, Struve M, Sharma A, Marini F, Mann A, Smith SA, Kaya Z, Strobl B, Mueller M, Reinhardt C, Morrissey JH, Bosmann M. 2020. Bacterial polyphosphates interfere with the innate host defense to infection. *Nat Commun* 11:4035. <https://doi.org/10.1038/s41467-020-17639-x>.
- Travers RJ, Smith SA, Morrissey JH. 2015. Polyphosphate, platelets, and coagulation. *Int J Lab Hematol* 37(Suppl 1):31–35. <https://doi.org/10.1111/ijlh.12349>.
- Gray MJ, Wholey WY, Wagner NO, Cremers CM, Mueller-Schickert A, Hock NT, Krieger AG, Smith EM, Bender RA, Bardwell JC, Jakob U. 2014. Polyphosphate is a primordial chaperone. *Mol Cell* 53:689–699. <https://doi.org/10.1016/j.molcel.2014.01.012>.
- Dahl JU, Gray MJ, Bazopoulou D, Beaufay F, Lempart J, Koenigsnecht MJ, Wang Y, Baker JR, Hasler WL, Young VB, Sun D, Jakob U. 2017. The anti-inflammatory drug mesalamine targets bacterial polyphosphate accumulation. *Nat Microbiol* 2:16267. <https://doi.org/10.1038/nmicrobiol.2016.267>.
- Xie L, Jakob U. 2019. Inorganic polyphosphate, a multifunctional polyanionic protein scaffold. *J Biol Chem* 294:2180–2190. <https://doi.org/10.1074/jbc.REV118.002808>.
- Bondy-Chorney E, Abramchuk I, Nasser R, Holinier C, Denoncourt A, Bajjal K, McCarthy L, Khacho M, Lavallee-Adam M, Downey M. 2020. A broad response to intracellular long-chain polyphosphate in human cells. *Cell Rep* 33:108318. <https://doi.org/10.1016/j.celrep.2020.108318>.
- Baev AY, Angelova PR, Abramov AY. 2020. Inorganic polyphosphate is produced and hydrolyzed in FOF1-ATP synthase of mammalian mitochondria. *Biochem J* 477:1515–1524. <https://doi.org/10.1042/BCJ20200042>.
- Gerasimaitė R, Mayer A. 2016. Enzymes of yeast polyphosphate metabolism: structure, enzymology and biological roles. *Biochem Soc Trans* 44:234–239. <https://doi.org/10.1042/BST20150213>.
- Kornberg A, Rao NN, Ault-Riche D. 1999. Inorganic polyphosphate: a molecule of many functions. *Annu Rev Biochem* 68:89–125. <https://doi.org/10.1146/annurev.biochem.68.1.89>.
- Auesukaree C, Homma T, Tochio H, Shirakawa M, Kaneko Y, Harashima S. 2004. Intracellular phosphate serves as a signal for the regulation of the PHO pathway in *Saccharomyces cerevisiae*. *J Biol Chem* 279:17289–17294. <https://doi.org/10.1074/jbc.M312202200>.
- Hothorn M, Neumann H, Lenherr ED, Wehner M, Rybin V, Hassa PO, Uttenweiler A, Reinhardt M, Schmidt A, Seiler J, Ladurner AG, Herrmann C, Scheffzek K, Mayer A. 2009. Catalytic core of a membrane-associated eukaryotic polyphosphate polymerase. *Science* 324:513–516. <https://doi.org/10.1126/science.1168120>.
- Gerasimaitė R, Sharma S, Desfougères Y, Schmidt A, Mayer A. 2014. Coupled synthesis and translocation restrains polyphosphate to acidocalcisome-like vacuoles and prevents its toxicity. *J Cell Sci* 127:5093–5104. <https://doi.org/10.1242/jcs.159772>.
- Denoncourt A, Downey M. 2021. Model systems for studying polyphosphate biology: a focus on microorganisms. *Curr Genet* 67:331–346. <https://doi.org/10.1007/s00294-020-01148-x>.
- Uttenweiler A, Schwarz H, Neumann H, Mayer A. 2007. The vacuolar transporter chaperone (VTC) complex is required for microautophagy. *Mol Biol Cell* 18:166–175. <https://doi.org/10.1091/mbc.e06-08-0664>.
- Muller O, Bayer MJ, Peters C, Andersen JS, Mann M, Mayer A. 2002. The Vtc proteins in vacuole fusion: coupling NSF activity to V(0) trans-complex formation. *EMBO J* 21:259–269. <https://doi.org/10.1093/emboj/21.3.259>.
- Muller O, Neumann H, Bayer MJ, Mayer A. 2003. Role of the Vtc proteins in V-ATPase stability and membrane trafficking. *J Cell Sci* 116:1107–1115. <https://doi.org/10.1242/jcs.00328>.
- Eskes E, Deprez MA, Wilms T, Winderickx J. 2018. pH homeostasis in yeast; the phosphate perspective. *Curr Genet* 64:155–161. <https://doi.org/10.1007/s00294-017-0743-2>.
- Nguyen TQ, Dziuba N, Lindahl PA. 2019. Isolated *Saccharomyces cerevisiae* vacuoles contain low-molecular-mass transition-metal polyphosphate complexes. *Metallomics* 11:1298–1309. <https://doi.org/10.1039/c9mt00104b>.
- Trilisenko L, Zvonarev A, Valiakhmetov A, Penin AA, Eliseeva IA, Ostroumov V, Kulakovskiy IV, Kulakovskaya T. 2019. The reduced level of inorganic polyphosphate mobilizes antioxidant and manganese-resistance systems in *Saccharomyces cerevisiae*. *Cells* 8:461. <https://doi.org/10.3390/cells8050461>.
- Ryazanova L, Zvonarev A, Rusakova T, Dmitriev V, Kulakovskaya T. 2016. Manganese tolerance in yeasts involves polyphosphate, magnesium, and vacuolar alterations. *Folia Microbiol (Praha)* 61:311–317. <https://doi.org/10.1007/s12223-015-0440-9>.
- Desfougères Y, Gerasimaitė RU, Jessen HJ, Mayer A. 2016. Vtc5, a novel subunit of the vacuolar transporter chaperone complex, regulates polyphosphate synthesis and phosphate homeostasis in yeast. *J Biol Chem* 291:22262–22275. <https://doi.org/10.1074/jbc.M116.746784>.
- Huang D, Moffat J, Andrews B. 2002. Dissection of a complex phenotype by functional genomics reveals roles for the yeast cyclin-dependent protein kinase Pho85 in stress adaptation and cell integrity. *Mol Cell Biol* 22:5076–5088. <https://doi.org/10.1128/MCB.22.14.5076-5088.2002>.
- Ogawa N, DeRisi J, Brown PO. 2000. New components of a system for phosphate accumulation and polyphosphate metabolism in *Saccharomyces cerevisiae* revealed by genomic expression analysis. *Mol Biol Cell* 11:4309–4321. <https://doi.org/10.1091/mbc.11.12.4309>.
- Gerasimaitė R, Pavlovic I, Capolicchio S, Hofer A, Schmidt A, Jessen HJ, Mayer A. 2017. Inositol pyrophosphate specificity of the SPX-dependent polyphosphate polymerase VTC. *ACS Chem Biol* 12:648–653. <https://doi.org/10.1021/acscchembio.7b00026>.
- Wild R, Gerasimaitė R, Jung JY, Truffault V, Pavlovic I, Schmidt A, Saiardi A, Jessen HJ, Poirier Y, Hothorn M, Mayer A. 2016. Control of eukaryotic phosphate homeostasis by inositol polyphosphate sensor domains. *Science* 352:986–990. <https://doi.org/10.1126/science.aad9858>.
- Azevedo C, Livermore T, Saiardi A. 2015. Protein polyphosphorylation of lysine residues by inorganic polyphosphate. *Mol Cell* 58:71–82. <https://doi.org/10.1016/j.molcel.2015.02.010>.
- Lonetti A, Sziogyarto Z, Bosch D, Loss O, Azevedo C, Saiardi A. 2011. Identification of an evolutionarily conserved family of inorganic polyphosphate endopolyphosphatases. *J Biol Chem* 286:31966–31974. <https://doi.org/10.1074/jbc.M111.266320>.

29. Beltrao P, Albanese V, Kenner LR, Swaney DL, Burlingame A, Villen J, Lim WA, Fraser JS, Frydman J, Krogan NJ. 2012. Systematic functional prioritization of protein posttranslational modifications. *Cell* 150:413–425. <https://doi.org/10.1016/j.cell.2012.05.036>.
30. Holt LJ, Tuch BB, Villen J, Johnson AD, Gygi SP, Morgan DO. 2009. Global analysis of Cdk1 substrate phosphorylation sites provides insights into evolution. *Science* 325:1682–1686. <https://doi.org/10.1126/science.1172867>.
31. Albuquerque CP, Smolka MB, Payne SH, Bafna V, Eng J, Zhou H. 2008. A multidimensional chromatography technology for in-depth phosphoproteome analysis. *Mol Cell Proteomics* 7:1389–1396. <https://doi.org/10.1074/mcp.M700468-MCP200>.
32. Feyder S, De Craene JO, Bar S, Bertazzi DL, Friant S. 2015. Membrane trafficking in the yeast *Saccharomyces cerevisiae* model. *Int J Mol Sci* 16:1509–1525. <https://doi.org/10.3390/ijms16011509>.
33. Ammann S, Schulz A, Krageloh-Mann I, Dieckmann NM, Niethammer K, Fuchs S, Eckl KM, Plank R, Werner R, Altmüller J, Thiele H, Nürnberg P, Bank J, Strauss A, von Bernuth H, Zur Stadt U, Grieve S, Griffiths GM, Lehmeberg K, Hennies HC, Ehl S. 2016. Mutations in AP3D1 associated with immunodeficiency and seizures define a new type of Hermansky-Pudlak syndrome. *Blood* 127:997–1006. <https://doi.org/10.1182/blood-2015-09-671636>.
34. El-Chemaly S, Young LR. 2016. Hermansky-Pudlak syndrome. *Clin Chest Med* 37:505–511. <https://doi.org/10.1016/j.ccm.2016.04.012>.
35. Huizing M, Malicdan MCV, Wang JA, Pri-Chen H, Hess RA, Fischer R, O'Brien KJ, Merideth MA, Gahl WA, Gochuico BR. 2020. Hermansky-Pudlak syndrome: mutation update. *Hum Mutat* 41:543–580. <https://doi.org/10.1002/humu.23968>.
36. Ruiz FA, Lea CR, Oldfield E, Docampo R. 2004. Human platelet dense granules contain polyphosphate and are similar to acidocalcisomes of bacteria and unicellular eukaryotes. *J Biol Chem* 279:44250–44257. <https://doi.org/10.1074/jbc.M406261200>.
37. Puy C, Tucker EI, Wong ZC, Gailani D, Smith SA, Choi SH, Morrissey JH, Gruber A, McCarty OJ. 2013. Factor XII promotes blood coagulation independent of factor XI in the presence of long-chain polyphosphates. *J Thromb Haemost* 11:1341–1352. <https://doi.org/10.1111/jth.12295>.
38. Choi SH, Smith SA, Morrissey JH. 2011. Polyphosphate is a cofactor for the activation of factor XI by thrombin. *Blood* 118:6963–6970. <https://doi.org/10.1182/blood-2011-07-368811>.
39. Choi SH, Smith SA, Morrissey JH. 2015. Polyphosphate accelerates factor V activation by factor XIa. *Thromb Haemost* 113:599–604. <https://doi.org/10.1160/TH14-06-0515>.
40. Smith SA, Mutch NJ, Baskar D, Rohloff P, Docampo R, Morrissey JH. 2006. Polyphosphate modulates blood coagulation and fibrinolysis. *Proc Natl Acad Sci U S A* 103:903–908. <https://doi.org/10.1073/pnas.0507195103>.
41. Muller F, Mutch NJ, Schenk WA, Smith SA, Esterl L, Spronk HM, Schmidbauer S, Gahl WA, Morrissey JH, Renne T. 2009. Platelet polyphosphates are proinflammatory and procoagulant mediators in vivo. *Cell* 139:1143–1156. <https://doi.org/10.1016/j.cell.2009.11.001>.
42. Bryant NJ, Stevens TH. 1998. Vacuole biogenesis in *Saccharomyces cerevisiae*: protein transport pathways to the yeast vacuole. *Microbiol Mol Biol Rev* 62:230–247. <https://doi.org/10.1128/MMBR.62.1.230-247.1998>.
43. Odorizzi G, Cowles CR, Emr SD. 1998. The AP-3 complex: a coat of many colours. *Trends Cell Biol* 8:282–288. [https://doi.org/10.1016/s0962-8924\(98\)01295-1](https://doi.org/10.1016/s0962-8924(98)01295-1).
44. Cowles CR, Odorizzi G, Payne GS, Emr SD. 1997. The AP-3 adaptor complex is essential for cargo-selective transport to the yeast vacuole. *Cell* 91:109–118. [https://doi.org/10.1016/s0092-8674\(01\)80013-1](https://doi.org/10.1016/s0092-8674(01)80013-1).
45. Azevedo C, Saiardi A. 2016. The new world of inorganic polyphosphates. *Biochem Soc Trans* 44:13–17. <https://doi.org/10.1042/BST20150210>.
46. Bentley-DeSousa A, Downey M. 2019. From underlying chemistry to therapeutic potential: open questions in the new field of lysine polyphosphorylation. *Curr Genet* 65:57–64. <https://doi.org/10.1007/s00294-018-0854-4>.
47. McCarthy L, Bentley-DeSousa A, Denoncourt A, Tseng YC, Gabriel M, Downey M. 2020. Proteins required for vacuolar function are targets of lysine polyphosphorylation in yeast. *FEBS Lett* 594:21–30. <https://doi.org/10.1002/1873-3468.13588>.
48. Bentley-DeSousa A, Holinier C, Moteshareie H, Tseng YC, Kajjo S, Nwosu C, Amodeo GF, Bondy-Chorney E, Sai Y, Rudner A, Golshani A, Davey NE, Downey M. 2018. A screen for candidate targets of lysine polyphosphorylation uncovers a conserved network implicated in ribosome biogenesis. *Cell Rep* 22:3427–3439. <https://doi.org/10.1016/j.celrep.2018.02.104>.
49. Stepp JD, Huang K, Lemmon SK. 1997. The yeast adaptor protein complex, AP-3, is essential for the efficient delivery of alkaline phosphatase by the alternate pathway to the vacuole. *J Cell Biol* 139:1761–1774. <https://doi.org/10.1083/jcb.139.7.1761>.
50. Ruotolo R, Marchini G, Ottonello S. 2008. Membrane transporters and protein traffic networks differentially affecting metal tolerance: a genomic phenotyping study in yeast. *Genome Biol* 9:R67. <https://doi.org/10.1186/gb-2008-9-4-r67>.
51. Kapitzky L, Beltrao P, Berens TJ, Gassner N, Zhou C, Wuster A, Wu J, Babu MM, Elledge SJ, Toczyski D, Lokey RS, Krogan NJ. 2010. Cross-species chemogenomic profiling reveals evolutionarily conserved drug mode of action. *Mol Syst Biol* 6:451. <https://doi.org/10.1038/msb.2010.107>.
52. Rehling P, Darsow T, Katzmann DJ, Emr SD. 1999. Formation of AP-3 transport intermediates requires Vps41 function. *Nat Cell Biol* 1:346–353. <https://doi.org/10.1038/14037>.
53. Angers CG, Merz AJ. 2009. HOPS interacts with Apl5 at the vacuole membrane and is required for consumption of AP-3 transport vesicles. *Mol Biol Cell* 20:4563–4574. <https://doi.org/10.1091/mbc.e09-04-0272>.
54. Chalfie M, Tu Y, Euskirchen G, Ward WW, Prasher DC. 1994. Green fluorescent protein as a marker for gene expression. *Science* 263:802–805. <https://doi.org/10.1126/science.8303295>.
55. Li M, Rong Y, Chuang YS, Peng D, Emr SD. 2015. Ubiquitin-dependent lysosomal membrane protein sorting and degradation. *Mol Cell* 57:467–478. <https://doi.org/10.1016/j.molcel.2014.12.012>.
56. Pokrzywa W, Guerriat B, Dodzian J, Morsomme P. 2009. Dual sorting of the *Saccharomyces cerevisiae* vacuolar protein Sna4p. *Eukaryot Cell* 8:278–286. <https://doi.org/10.1128/EC.00363-08>.
57. Reggiori F, Klionsky DJ. 2013. Autophagic processes in yeast: mechanism, machinery and regulation. *Genetics* 194:341–361. <https://doi.org/10.1534/genetics.112.149013>.
58. Henne WM, Buchkovich NJ, Emr SD. 2011. The ESCRT pathway. *Dev Cell* 21:77–91. <https://doi.org/10.1016/j.devcel.2011.05.015>.
59. Schmidt O, Teis D. 2012. The ESCRT machinery. *Curr Biol* 22:R116–R120. <https://doi.org/10.1016/j.cub.2012.01.028>.
60. Hecht KA, O'Donnell AF, Brodsky JL. 2014. The proteolytic landscape of the yeast vacuole. *Cell Logist* 4:e28023. <https://doi.org/10.4161/cl.28023>.
61. Freimoser FM, Hurlimann HC, Jakob CA, Werner TP, Amrhein N. 2006. Systematic screening of polyphosphate (poly P) levels in yeast mutant cells reveals strong interdependence with primary metabolism. *Genome Biol* 7:R109. <https://doi.org/10.1186/gb-2006-7-11-r109>.
62. Park SY, Guo X. 2014. Adaptor protein complexes and intracellular transport. *Biosci Rep* 34:e00123. <https://doi.org/10.1042/BSR20140069>.
63. Darsow T, Katzmann DJ, Cowles CR, Emr SD. 2001. Vps41p function in the alkaline phosphatase pathway requires homo-oligomerization and interaction with AP-3 through two distinct domains. *Mol Biol Cell* 12:37–51. <https://doi.org/10.1091/mbc.12.1.37>.
64. Schoppe J, Mari M, Yavavli E, Auffarth K, Cabrera M, Walter S, Frohlich F, Ungermann C. 2020. AP-3 vesicle uncoating occurs after HOPS-dependent vacuole tethering. *EMBO J* 39:e105117. <https://doi.org/10.15252/emboj.2020105117>.
65. Cabrera M, Langemeyer L, Mari M, Rethmeier R, Orban I, Perz A, Broucker C, Griffith J, Klose D, Steinhoff HJ, Reggiori F, Engelbrecht-Vandre S, Ungermann C. 2010. Phosphorylation of a membrane curvature-sensing motif switches function of the HOPS subunit Vps41 in membrane tethering. *J Cell Biol* 191:845–859. <https://doi.org/10.1083/jcb.201004092>.
66. Mechler B, Muller M, Muller H, Meussdoerffer F, Wolf DH. 1982. In vivo biosynthesis of the vacuolar proteinases A and B in the yeast *Saccharomyces cerevisiae*. *J Biol Chem* 257:11203–11206. [https://doi.org/10.1016/S0021-9258\(18\)33740-2](https://doi.org/10.1016/S0021-9258(18)33740-2).
67. Distel B, Al EJ, Tabak HF, Jones EW. 1983. Synthesis and maturation of the yeast vacuolar enzymes carboxypeptidase Y and aminopeptidase I. *Biochim Biophys Acta* 741:128–135. [https://doi.org/10.1016/0167-4781\(83\)90019-2](https://doi.org/10.1016/0167-4781(83)90019-2).
68. Reggiori F, Pelham HR. 2001. Sorting of proteins into multivesicular bodies: ubiquitin-dependent and -independent targeting. *EMBO J* 20:5176–5186. <https://doi.org/10.1093/emboj/20.18.5176>.
69. Swaminathan S, Amerik AY, Hochstrasser M. 1999. The Doa4 deubiquitinating enzyme is required for ubiquitin homeostasis in yeast. *Mol Biol Cell* 10:2583–2594. <https://doi.org/10.1091/mbc.10.8.2583>.
70. Oughtred R, Stark C, Breitkreutz BJ, Rust J, Boucher L, Chang C, Kolas N, O'Donnell L, Leung G, McAdam R, Zhang F, Dolma S, Willems A, Coulombe-Huntington J, Chatr-Aryamontri A, Dolinski K, Tyers M. 2019. The BioGRID interaction database: 2019 update. *Nucleic Acids Res* 47:D529–D541. <https://doi.org/10.1093/nar/gky1079>.
71. Stringer DK, Piper RC. 2011. A single ubiquitin is sufficient for cargo protein entry into MVBs in the absence of ESCRT ubiquitination. *J Cell Biol* 192:229–242. <https://doi.org/10.1083/jcb.201008121>.

72. Zhu L, Jorgensen JR, Li M, Chuang YS, Emr SD. 2017. ESCRTs function directly on the lysosome membrane to downregulate ubiquitinated lysosomal membrane proteins. *Elife* 6:e26403. <https://doi.org/10.7554/eLife.26403>.
73. McNatt MW, McKittrick I, West M, Odorizzi G. 2007. Direct binding to Rsp5 mediates ubiquitin-independent sorting of Sna3 via the multivesicular body pathway. *Mol Biol Cell* 18:697–706. <https://doi.org/10.1091/mbc.e06-08-0663>.
74. Llinares E, Barry AO, Andre B. 2015. The AP-3 adaptor complex mediates sorting of yeast and mammalian PQ-loop-family basic amino acid transporters to the vacuolar/lysosomal membrane. *Sci Rep* 5:16665. <https://doi.org/10.1038/srep16665>.
75. Bru S, Jimenez J, Canadell D, Arino J, Clotet J. 2016. Improvement of biochemical methods of polyP quantification. *Microb Cell* 4:6–15. <https://doi.org/10.15698/mic2017.01.551>.